

## Entropy engineering in inorganic non-metallic glass

Feng, X.; Yue, Yuanzheng; Qiu, J.R.; Jain, H.; Zhou, S.F.

*Published in:*  
Fundamental Research

*DOI (link to publication from Publisher):*  
[10.1016/j.fmre.2022.01.030](https://doi.org/10.1016/j.fmre.2022.01.030)

*Creative Commons License*  
CC BY-NC-ND 4.0

*Publication date:*  
2022

*Document Version*  
Publisher's PDF, also known as Version of record

[Link to publication from Aalborg University](#)

*Citation for published version (APA):*  
Feng, X., Yue, Y., Qiu, J. R., Jain, H., & Zhou, S. F. (2022). Entropy engineering in inorganic non-metallic glass. *Fundamental Research*, 2(5), 783–793. <https://doi.org/10.1016/j.fmre.2022.01.030>

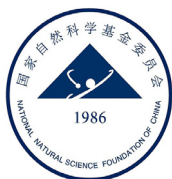
### General rights

Copyright and moral rights for the publications made accessible in the public portal are retained by the authors and/or other copyright owners and it is a condition of accessing publications that users recognise and abide by the legal requirements associated with these rights.

- Users may download and print one copy of any publication from the public portal for the purpose of private study or research.
- You may not further distribute the material or use it for any profit-making activity or commercial gain
- You may freely distribute the URL identifying the publication in the public portal -

### Take down policy

If you believe that this document breaches copyright please contact us at [vbn@aub.aau.dk](mailto:vbn@aub.aau.dk) providing details, and we will remove access to the work immediately and investigate your claim.



## Review

## Entropy engineering in inorganic non-metallic glass

Xu Feng<sup>a,b</sup>, Yuanzheng Yue<sup>c</sup>, Jianrong Qiu<sup>d</sup>, Himanshu Jain<sup>e</sup>, Shifeng Zhou<sup>a,b,\*</sup><sup>a</sup> State Key Laboratory of Luminescent Materials and Devices, School of Materials Science and Engineering, South China University of Technology, Guangzhou 510640, China<sup>b</sup> Guangdong Provincial Key Laboratory of Fiber Laser Materials and Applied Techniques, Guangdong Engineering Technology Research and Development Center of Special Optical Fiber Materials and Devices, Guangzhou 510640, China<sup>c</sup> Department of Chemistry and Bioscience, Aalborg University, Aalborg 9220, Denmark<sup>d</sup> College of Optical Science and Engineering, Zhejiang University, Hangzhou 310027, China<sup>e</sup> Department of Materials Science and Engineering, Lehigh University, Bethlehem PA 18015, United States

## ARTICLE INFO

## Article history:

Received 21 October 2021

Received in revised form 2 January 2022

Accepted 23 January 2022

Available online 17 February 2022

## Keywords:

Entropy engineering

Inorganic non-metallic glass

Glass formation

Microstructure

Properties

## ABSTRACT

Advances in developing high entropy alloys and ceramics with improved physical properties have greatly broadened their application field from aerospace industry, public transportation to nuclear plants. In this review, we describe the concept of entropy engineering as applicable to inorganic non-metallic glasses, especially for tailoring and enhancing their mechanical, electrical, and optical properties. We also present opportunities and challenges in calculating entropy of inorganic non-metallic glass systems, correlating entropy to glass formation, and in developing functional inorganic non-metallic glasses via the entropy concept.

## 1. Introduction

Entropy is an extensive property of a thermodynamic system. It is associated with the confusion degree in a system, along with macroscopic thermodynamic quantities such as volume, pressure, and temperature. For a specific material system, entropy can be mainly of two origins: vibrational and configurational, representing the degree of disorder due to the vibration of molecules, atoms or ions and the diversification of the structural configurations, respectively. In recent years, the entropy engineering concept has been used as an effective way to tune the thermodynamic and physical properties of materials. This concept was proposed by Yeh et al. in 2004 [1] with the purpose to develop novel alloys. The core of the concept is to increase the configurational entropy of an alloy by mixing multiple equimolar or near-equimolar metal elements, thereby to improve its performance. Specially, the alloys with more than five equimolar or near-equimolar base elements are defined as “high entropy alloys” [1,2], which would form single-phase alloys rather than multi-phase mixture of intercrystalline compounds. Over the past seventeen years, the high entropy alloy has been extensively studied and a series of material systems with face-center [3–8], body-center cubic [9–11] and hexagonal close packed [12–15] solid solution structure

has been fabricated. In addition to high entropy crystalline alloys, high-entropy amorphous alloys (metallic glasses) [16–20] have also been developed by using the concept of entropy engineering. Benefitting from the unique structure, the high entropy alloys exhibit excellent mechanical properties such as high strength [12,21], high corrosion resistance [22] and exceptional fracture toughness [23–25]. Motivated by the substantial progress in the field of high entropy alloys, the entropy engineering concept was further employed to develop novel ceramics [26]. The high entropy ceramics, including oxides [27–31], carbides [32–35], diborides [36–39] and silicides [40,41], have been synthesized, which exhibit remarkable properties such as high hardness [42], high corrosion resistance [43,44], and low thermal conductivity [45,46] compared to conventional ceramics.

As illustrated in Fig. 1a–c, in contrast to metals and ceramics, multicomponent inorganic non-metallic glasses (e.g., oxide, chalcogenide, and fluoride glasses) feature a more complicated microstructure owing to the long-range disordered network consisting of various kinds of local-range and intermediate-range structural units [47]. For this reason, these glasses can be regarded as high entropy systems. The configurational entropy of glasses is higher than that of its crystalline counterpart since there is a larger fluctuation in both bond length and bond an-

\* Corresponding author.

E-mail address: [zhoushifeng@scut.edu.cn](mailto:zhoushifeng@scut.edu.cn) (S. Zhou).

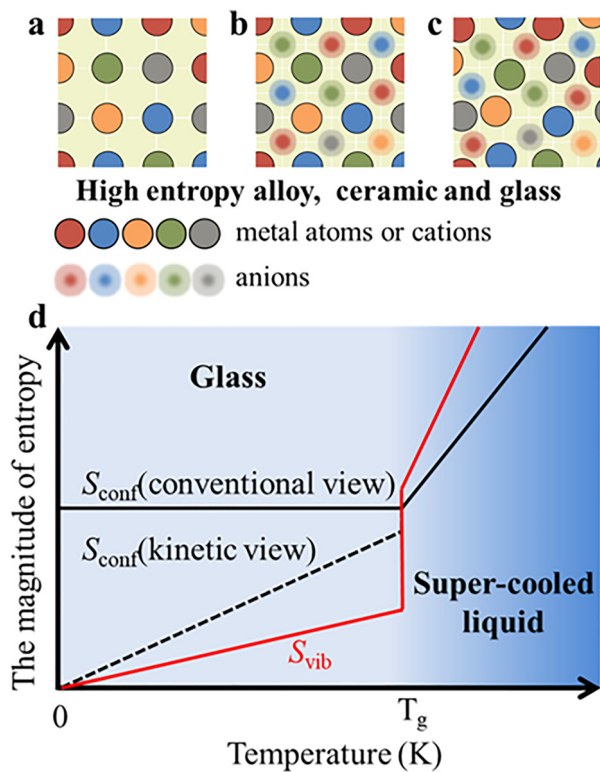


Fig. 1. Schematic illustration of the arrangement of component elements (as represented by the circles in different colors) in the (a) high entropy alloys, (b) high entropy ceramics, and (c) high entropy inorganic non-metallic glasses. (d) The entropy evolution during glass formation.

gles of the structural units. Furthermore, the entropy contributed from the diversity of composition in multicomponent glasses is believed to be greater than that in alloys and ceramics. The components of inorganic non-metallic glasses can be divided into network formers (e.g.,  $\text{SiO}_2$ ,  $\text{GeO}_2$ ,  $\text{P}_2\text{O}_5$ , and  $\text{B}_2\text{O}_3$ ), network modifiers (e.g.,  $\text{Li}_2\text{O}$ ,  $\text{Na}_2\text{O}$ , and  $\text{K}_2\text{O}$ ), and network intermediates (e.g.,  $\text{Al}_2\text{O}_3$ ,  $\text{Ga}_2\text{O}_3$ , and  $\text{ZnO}$ ). Thus, we can introduce the concept of entropy engineering into the field of inorganic non-metallic glasses, and thereby design novel glasses with higher entropy. It should be noted that, to the best of our knowledge, the entropy engineering concept has not been purposely introduced and applied for investigating and developing inorganic non-metallic glasses.

In this review, we establish the entropy engineering concept regarding inorganic non-metallic glasses. We describe the route to calculate the entropy of inorganic non-metallic glasses and provide insight into the influence of entropy on physical properties of inorganic non-metallic glasses. We describe the potential applications and challenges of the entropy engineering strategy for developing novel inorganic non-metallic glasses.

## 2. The concept of entropy in inorganic non-metallic glass

According to the definition proposed by Boltzmann, entropy  $S$  is usually considered as the measure of the system's disorder, which can be expressed as (at 0 K):

$$S = k \ln \Omega \quad (1)$$

where  $k$  is the Boltzmann constant and  $\Omega$  is the number of microstates. Clausius proposed that for a reversible process, the change in entropy ( $dS$ ) is given by the second law of thermodynamics:

$$dS = \frac{\delta Q}{T} \quad (2)$$

where  $Q$  is the heat supplied to the system and  $T$  is temperature. For a system of matter (e.g., alloys, ceramics, and glasses), the degree of the

disorder can be described by both the configurational entropy ( $S_{\text{conf}}$ ) and the vibrational entropy ( $S_{\text{vib}}$ ). Thus, the total entropy of a material system may be expressed as:

$$S = S_{\text{conf}} + S_{\text{vib}} \quad (3)$$

where  $S_{\text{conf}}$  is mainly determined by the number of components and the number of structural arrangements. An increase of these numbers could lead to higher  $S_{\text{conf}}$ .  $S_{\text{vib}}$  is mainly determined by the intrinsic vibrational properties of the composed molecules, atoms, or ions. Both  $S_{\text{conf}}$  and  $S_{\text{vib}}$  are temperature dependent in different fashions as discussed elsewhere [48,49]. For a solid state (such as alloys, ceramics, and glasses) system,  $S_{\text{conf}}$  is thought to dominate the total  $S$  of the system [50]. Thus, this article mainly focuses on the contribution of  $S_{\text{conf}}$ .

In recent years, the configurational entropy engineering strategy has been proposed with respect to alloy and ceramic materials through multicomponent mixing. The  $\Delta S_{\text{conf}}$  of a system (e.g., alloys and ceramics) due to multicomponent mixing is usually measured by mixed entropy ( $\Delta S_{\text{mix}}$ ). In classical equilibrium thermodynamics, the  $\Delta S_{\text{mix}}$  is defined as the increase in the total entropy ( $\Delta S$ ) when several initially separated equilibrium systems with different components are mixed without chemical reaction to a new thermodynamic internal equilibrium system. For a typical equilibrium system (e.g., alloys and ceramics), the relation between  $\Delta S_{\text{conf}}$  and  $\Delta S_{\text{mix}}$  after  $n$  components mixing (ignoring the contribution of  $S_{\text{vib}}$ ) can be given as [1,15]:

$$\begin{aligned} \Delta S_{\text{conf}} &= S_{\text{conf}}(\text{mixed system}) - \sum_{k=1}^n S_{\text{conf}}(k^{\text{th}} \text{ separated system}) \approx \Delta S_{\text{mix}} \\ &= \Delta S = S(\text{mixed system}) - \sum_{k=1}^n S(k^{\text{th}} \text{ separated system}) \end{aligned} \quad (4)$$

Thus,  $S_{\text{conf}}$  is tuned via changing the component elements, and multicomponent mixing is expected to generate additional configurational entropy. As modelled for the ideal solid solution,  $\Delta S_{\text{conf}}$  in alloys and ceramics can be simply calculated through Eqs. 5 and 6, respectively [1,15,51]:

$$\Delta S_{\text{conf}} = \Delta S_{\text{mix}} = -R \sum_{i=1}^N c_i \ln c_i \quad (5)$$

where  $R$  is the gas constant, which is the product of Avagadro constant  $N_A$  and Boltzmann constant  $k$ , and  $c_i$  is the molar fraction of the  $i^{\text{th}}$  metal element.

$$\Delta S_{\text{conf}} = \Delta S_{\text{mix}} = -R \left[ \frac{X}{X+Y} \sum_{i=1}^{N_h} x_i^h \ln(x_i^h) + \frac{Y}{X+Y} \sum_{i=1}^{N_k} x_i^k \ln(x_i^k) \right] \quad (6)$$

where  $X$  and  $Y$  are total number of the ions occupying  $h$  and  $k$  sublattices,  $N_h$  and  $N_k$  are the number of species occupying  $h$  and  $k$  sites, and  $x_i^h$  and  $x_i^k$  are the molar fraction of the  $i^{\text{th}}$  element that occupies  $h$  and  $k$  sites. According to Eqs. 5, 6, it can be shown that multicomponent system, especially equimolar mixed materials, would exhibit higher  $S_{\text{conf}}$  than the separated systems.

As for inorganic non-metallic glasses, which are the non-equilibrium systems, the ideal equilibrium solid solution model is not suitable for the estimation of  $\Delta S_{\text{conf}}$ . Taking the melt-quenched non-equilibrium glass system as the typical example, the evolution of  $S_{\text{vib}}$  and  $S_{\text{conf}}$  in the whole process from melt state to solid state should be re-analyzed (Fig. 1d). During glass formation,  $S_{\text{vib}}$  sharply decreases and its contribution to the total change of entropy in the glassy state can be neglected. Instead,  $S_{\text{conf}}$  dominates, and  $S$  approximately equals  $S_{\text{conf}}$ :

$$S \approx S_{\text{conf}} \quad (7)$$

In principle,  $S_{\text{conf}}$  of an inorganic non-metallic glass system is regarded as the frozen  $S_{\text{conf}}$  from the super-cooled liquid at a certain fictive temperature [52]. In details,  $S_{\text{conf}}$  in inorganic non-metallic glasses would be related not only to its composition but also to its thermal history during transformation from the liquid melt to the glassy phase.

Table 1

The comparison of entropy engineering strategies by component diversification in alloys, ceramics and inorganic non-metallic glasses.

	Phase evolution	Diversified components	Component occupation
Alloys	Single phase solid solution	Mainly the metal atoms	Specific Wyckoff site for metal atoms
Ceramics	Single phase solid solution	Cations or anions with the same or similar chemical valence	Specific Wyckoff site for cations or anions
Inorganic non-metallic glasses	Single phase	Cations or anions with fewer limits	Unspecific sites

There are two conflicting theoretical models for describing frozen  $S_{\text{conf}}$  [49,53–60]. According to the conventional view, all the  $S_{\text{conf}}$  would be frozen during glass transition and non-zero residual  $S_{\text{conf}}$  at 0 K would be observed. Alternatively, the kinetic view considers the occurrence of an entropy loss during the transition from the liquid to glass and the residual  $S_{\text{conf}}$  vanishes at 0 K. Both views agree that faster cooling rate during glass transition leads to higher  $S_{\text{conf}}$  in inorganic non-metallic glasses [52]. Thus,  $S_{\text{conf}}$  of inorganic non-metallic glasses is thermal history dependent [61]. For a certain thermal history,  $S_{\text{conf}}$  of inorganic non-metallic glasses can be expressed as [56]:

$$S_{\text{conf}} = -k \sum_{i=1}^N \text{Tr}[p_i \ln(p_i)] \quad (8)$$

where  $p_i$  is the density matrix of the  $i^{\text{th}}$  microstate of total  $N$  of the system and  $\text{Tr}$  is its trace.

Thus, for mixed non-equilibrium system, such as inorganic non-metallic glasses, the change of the total entropy is caused by both the diversification of the components and the quenching process (the thermal history for inorganic glass). So, the change of total entropy can be calculated via:

$$\begin{aligned} \Delta S &= S(\text{mixed system}) - \sum_{k=1}^n S(k^{\text{th}} \text{ separated system}) \\ &\approx S_{\text{conf}}(\text{mixed system}) - \sum_{k=1}^n S_{\text{conf}}(k^{\text{th}} \text{ separated system}) = \Delta S_{\text{conf}} \\ &= \Delta S_{\text{mix}} + \Delta S'_{\text{conf}} \end{aligned} \quad (9)$$

where  $\Delta S$  is the total entropy change,  $\Delta S_{\text{conf}}$  is the configurational entropy change,  $\Delta S_{\text{mix}}$  is the mixed entropy,  $\Delta S'_{\text{conf}}$  is the configurational entropy change due to quenching process for a non-equilibrium system.

Based on above description, it is reasonable that the configurational entropy engineering concept can be extended from the field of alloys and ceramics to that of inorganic non-metallic glasses. Like ceramics and alloys, multicomponent mixed glass system may exhibit higher  $S_{\text{conf}}$  than that of its subsystem due to the positive  $\Delta S_{\text{mix}}$ . However, Compared to the equilibrium systems such as ceramics and alloys,  $S_{\text{conf}}$  of the non-equilibrium inorganic non-metallic glasses can be adjusted through thermal history manipulation. Faster cooling rate during glass formation is another approach for raising  $S_{\text{conf}}$  due to the positive  $\Delta S'_{\text{conf}}$ . For instance, the hyperquenched glasses (cooling at a rate of  $10^6$  K/s) exhibit more disordered local microstructure and significantly higher frozen entropy compared with those of the glass cooled at the standard cooling rate of 0.1 K/s [61–63]. Thus, thermal history (e.g., controlling cooling rate) is another controlling factor for the configurational entropy ( $\Delta S'_{\text{conf}}$ ) and physical properties of inorganic non-metallic glasses.

However, the precisely control of thermal history of inorganic non-metallic glasses is still a challenge. Here, the configurational entropy engineering for inorganic non-metallic glasses is discussed based on component diversification ( $\Delta S_{\text{mix}}$  design).

The crucial aspects of the entropy engineering concept, which is based on the component diversification, are demonstrated and compared for alloys, ceramics and inorganic non-metallic glasses as seen in Table 1. For alloys and ceramics, the final product of entropy engineering is a novel single-phase solid solution composed of various kinds of components. The diversification components, which are carefully selected to mitigate the enthalpic penalties, would occupy the specific Wyckoff site of the crystal cell units. The higher entropy solid solutions exhibit the same or similar crystal structure (e.g., space group)

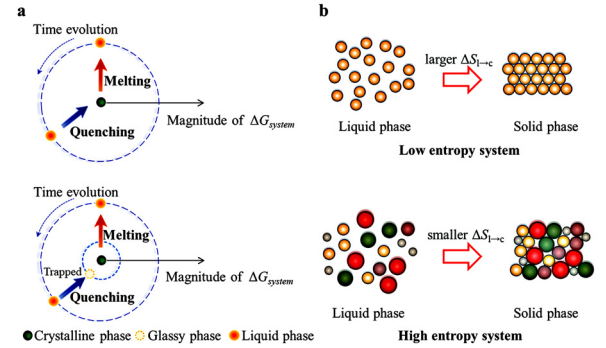


Fig. 2. Influence of entropy on glass formation. (a) Magnitude and phase profile of  $\Delta G_{\text{system}}$  in glass formation and crystallization process. (b) Schematic illustration of liquid phase and crystalline phase of low entropy system (top graph) and high entropy system (bottom graph).

compared with their lower entropy subsystems, but with larger local disorder. The unique physical properties of high entropy ceramic and alloy mainly result from the local disorder. As for inorganic non-metallic glasses, entropy engineering would lead to different topological structures from that of its lower entropy subsystems. A prominent feature of glass is that the diversification components can be selected with fewer limits and they are supposed not to occupy a specific site.

### 3. Mixed entropy design for control of glass formation

The process of materials synthesis is accompanied by the evolution of the Gibbs free energy of the system. According to the fundamental principles of statistical mechanics, the Gibbs free energy change of the system  $\Delta G_{\text{system}1 \rightarrow 2}$  can be calculated through:

$$\Delta G_{\text{system}1 \rightarrow 2} = \Delta H_{\text{system}1 \rightarrow 2} - T \Delta S_{\text{system}1 \rightarrow 2} \quad (10)$$

where  $\Delta H_{\text{system}1 \rightarrow 2}$  is the system enthalpy change,  $T$  is the temperature and  $\Delta S_{\text{system}1 \rightarrow 2}$  is the system entropy change. For high entropy alloys or ceramics, the Gibbs free energy difference  $\Delta G_{\text{separated} \rightarrow \text{mix}}$  between the separated intercrystalline phases and mixed multicomponent high entropy phase would be expressed as:

$$\Delta G_{\text{separated} \rightarrow \text{mix}} = \Delta H_{\text{mix}} - T \Delta S_{\text{mix}} \quad (11)$$

where  $\Delta H_{\text{mix}}$  is the mixed enthalpy. In comparison, at high temperature:

$$\Delta H_{\text{mix}} \ll T \Delta S_{\text{mix}} \quad (12)$$

which indicates that  $\Delta G_{\text{separated} \rightarrow \text{mix}}$  is negative and high entropy multicomponent ceramics and alloys exhibit lower Gibbs energy compared with that of the intercrystalline phases. The tendency of ordering and segregation would be lowered due to the entropy stabilized effect [15,26,64,65]. Thus, high entropy alloys or ceramics are more likely to form random mixed solid solution instead of intercrystalline phases during solidification.

Since the glass is a complicated non-equilibrium state that forms via the melt-quenching process (Fig. 2a), the contribution of  $\Delta S_{\text{mix}}$  to glass formation cannot be solely ascribed to the entropy stabilizing effect, in contrast to the cases in alloys and ceramics. In recent years, the contribution of  $\Delta S_{\text{mix}}$  to glass formation has been analyzed based on crystallization thermodynamics. Guided by the crystallography theory, the



total Gibbs energy difference ( $\Delta G_{l \rightarrow c}$ ) between the liquid and crystalline phase can be expressed as [66,67]:

$$\Delta G_{l \rightarrow c} = \frac{4}{3} \pi r^3 \Delta g_v + 4 \pi r^2 \sigma \quad (13)$$

where  $\Delta g_v$  and  $\sigma$  are the free energy change (driving force) and the interface energy change during the formation of the nuclei from the super-cooled liquid, respectively,  $r$  is the radius of nucleus. The critical nucleus radius  $r^*$  can be calculated by [68]:

$$\frac{d\Delta G_{l \rightarrow c}}{dr} = 0 \quad (14)$$

and further:

$$r^* = -\frac{2\sigma}{\Delta g_v} \quad (15)$$

The nucleus with  $r < r^*$  is unstable, indicating that the larger  $r^*$  may lead to higher glass formation ability. Making  $\Delta g_v$  less negative is the effective strategy to improve the glass formation ability. At constant pressure,  $\Delta g_v$  can be calculated by [69]:

$$\Delta g_v = \Delta S_{l \rightarrow c} \Delta T \frac{2T}{T_m + T} \quad (16)$$

where  $\Delta S_{l \rightarrow c}$  is the total entropy difference between liquid and crystalline phase at melting point, which is negative,  $T_m$  is the melting point,  $T$  is the actual temperature and  $\Delta T = T_m - T$  is the super-cooling degree. According to Eq. (16), less negative  $\Delta S_{l \rightarrow c}$  corresponds to lower tendency for crystallization, and hence, to higher glass forming ability (Fig. 2b).

It is established that the multicomponent mixed system (with higher  $\Delta S_{mix}$ ) exhibits less negative  $\Delta S_{l \rightarrow c}$  compared with that of the separated subsystem (with lower  $\Delta S_{mix}$ ) [69]. That is to say, the high mixed entropy system would exhibit a greater tendency to glass formation. This mixed entropy design strategy was called the “confusion by design” principle for the formation of metallic glass and has become one of the important empirical rules for designing metallic glasses [70]. Although a series of metallic glasses have been designed and fabricated, the “confusion by design” principle has not yet been strictly demonstrated and further studies still need to be done.

In addition, the contribution of  $\Delta S_{mix}$  to the glass formation has also been analyzed based on crystallization kinetic theory. In crystallization kinetic theory, glass formation ability is governed by the viscosity of the super-cooled liquid. In highly viscous state, the diffusion of atoms (or ions) can be effectively reduced and thus the nucleation and growth of the crystalline phase would be suppressed, finally leading to glass formation. According to the Adams-Gibbs model, the relation between  $S_{conf}$  and viscosity ( $\eta$ ) of liquid can be described by [60]:

$$\eta \propto \exp\left(\frac{A}{TS_{conf}}\right) \quad (17)$$

where  $A$  is a constant. The  $S_{conf}$  of the liquid can be determined by the Mauro-Yue-Ellison-Gupta-Allan (MYEGA) equation [49]. The Adams-Gibbs model suggests that high  $S_{conf}$  is inversely correlated with the viscosity of the liquid.

According to Eq. 4, for equilibrium liquid phase, we have the expression:

$$S_{conf}(\text{mixed system}) = \sum_{k=1}^n S_{conf}(k^{th} \text{ separated system}) + \Delta S_{mix} \quad (18)$$

Due to the positive  $\Delta S_{mix}$ , the multicomponent mixed system in equilibrium liquid state exhibits higher  $S_{conf}$ . Thus, based on crystallization kinetic theory, multicomponent glass systems with higher configurational entropy may accelerate crystallization and decrease the glass forming ability.

As for inorganic non-metallic glasses, the influence of entropy on glass stability is found to be three-fold. First, high entropy is beneficial to the formation of inorganic non-metallic glass in many cases. As a typical example, pure  $\text{TeO}_2$  cannot form glassy phase alone, due to its unstable network structure. Enhancement of  $\Delta S_{mix}$  via adding the network modifiers or intermediates such as  $\text{Na}_2\text{O}$ ,  $\text{Nb}_2\text{O}_5$  and  $\text{V}_2\text{O}_5$  can stabilize the

unstable structure and highly transparent functional tellurite glasses can be fabricated [71–75]. This is consistent with above theoretical analysis. Second, the high entropy strategy is not always feasible for improving glass formation. For example,  $\text{SiO}_2$  is one of the best network formers. However, increasing the entropy of the system via diversifying the composition (e.g., adding  $\text{Li}_2\text{O}$ ) will decrease the viscosity of the glass melt, resulting in the enhancement of the glass crystallization tendency. Third, the rational control of  $S_{conf}$  via  $\Delta S_{mix}$  design also facilitates the densification during glass formation. As another typical example,  $\text{B}_2\text{O}_3$  is a good glass former. However, it is unstable under ambient condition for long time due to its loose laminated network structure, i.e., it is easy to degrade. It has been demonstrated that the addition of  $\text{Al}_2\text{O}_3$  and  $\text{Na}_2\text{O}$  can promote the transformation of the loose laminated structure into the dense three-dimensional network structure, contributing to the formation of the stable borate glass system [76–78]. Thus, entropy engineering provides an effective avenue to tune glass formation and glass stability, and thus, high quality glass can be obtained by entropy engineering.

#### 4. Entropy engineering for control of glass properties

For high entropy ceramics and alloys, besides the direct high entropy effect (entropy stabilized effect), entropy engineering also leads to indirect effects such as cocktail effect and sluggish kinetics, which are thought to be not related to entropy directly but the modification of local structure due to component diversification. These direct and indirect effects have been demonstrated to improve mechanical, electrical and magnetic properties of ceramics and alloys.

Although the high entropy effect of inorganic non-metallic glasses is yet to be established as a topic of glass science, various properties of inorganic non-metallic glasses have been found to be associated with  $S_{conf}$  or the resultant microstructure change due to component diversification. It is necessary to point out that the multicomponent glass systems account for a large proportion of commercial glass products. The established golden rule to tune the glass properties is based on component diversification. This strategy can be regarded as a cocktail effect or sluggish kinetics effect for inorganic non-metallic glass. In the following sections, several examples about the entropy-structure-property relation in various glass systems are highlighted.

##### 4.1. Mechanical properties

As is well known, entropic elasticity is the typical property of rubber above its glass transition temperature,  $T_g$ , since rubber is composed of crosslinked carbon chains. Under tension, the orientation of carbon chain (-C-C-) results in the structural anisotropy as well as the decrease of entropy of the system:  $S_{loading} < S_{origin}$ , which are the entropy under tension and in original state, respectively. After unloading, according to the second law of thermodynamics, the system should spontaneously evolve to the higher entropy state, and thus the oriented chains would shrink through micro-Brownian motion process. The crosslinking agent with the disulfide bonds that increases the inter-chain force can effectively suppress the macro-Brownian motion of the chains, thus allowing the chains to “memorize” the original position and finally the chains can recover to the initial state. This intriguing entropy-dominated process inspires us to propose a new question. That is, is it possible to gift rigid glass with entropic elasticity via entropy engineering? Based on the above analysis, the glass with structure like that of rubber, such as the metaphosphate glass that is composed of long P-O-P chains and alkali metal species as crosslink agent, might be a potential candidate for examining the entropy effect. Unfortunately, the entropic elasticity has never been observed in a simple glass composition e.g., the metaphosphate glass,  $50\text{Li}_2\text{O}-50\text{P}_2\text{O}_5$  (mol%) [79].

In recent years, Hosono et al. proposed that entropic elasticity cannot be generated in the metaphosphate glass with single alkali metal ions [80]. Keeping this key point in mind, they tried to in-

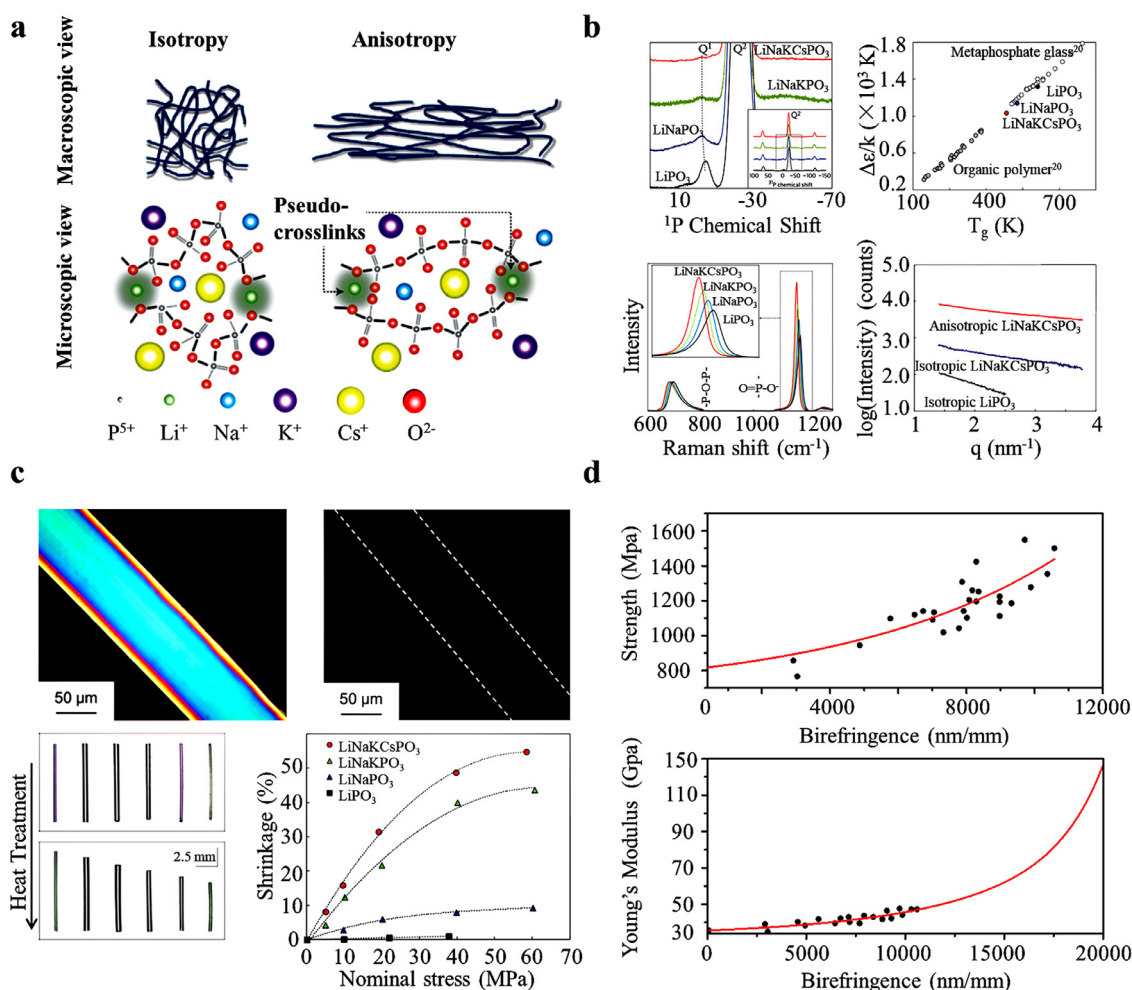


**Fig. 3. Entropy engineering for control of mechanical properties of glass [80,81].** (a) The model structure of multicomponent entropic elastic metaphosphate glass. (b) Structure features of the metaphosphate glass. Left: <sup>31</sup>P MAS NMR (top graph) and Raman spectra (bottom graph) of metaphosphate glass with different  $\Delta S_{\text{mix}}$  values. Right: Intermolecular energies of organic polymers and metaphosphate glass (top graph) and SAXS profiles for metaphosphate glass (bottom graph). (c) Upper panel: Polarization images of high entropic metaphosphate glass fiber before (left graph) and after (right graph) relaxation at  $T_g$ . Lower panel: Shrinkage of the high entropic metaphosphate glass (left graph) and composition dependence of entropic shrinkage of metaphosphate glasses. (d) Strength (Upper graph) and Young's modulus (Lower graph) of high entropic metaphosphate glass fiber.

corporate various types of alkali metal ions (Li, Na, K and Cs) into metaphosphate glass system to tune the entropy. They fabricated and studied four glass compositions (mol%): 50Li<sub>2</sub>O-50P<sub>2</sub>O<sub>5</sub>, 25Li<sub>2</sub>O-25Na<sub>2</sub>O-50P<sub>2</sub>O<sub>5</sub>, 16.6Li<sub>2</sub>O-16.6Na<sub>2</sub>O-16.6K<sub>2</sub>O-50P<sub>2</sub>O<sub>5</sub> and 12.5Li<sub>2</sub>O-12.5Na<sub>2</sub>O-12.5K<sub>2</sub>O-12.5Cs<sub>2</sub>O-50P<sub>2</sub>O<sub>5</sub>, which have different entropy values. It was found that at the temperature above  $T_g$  the elastic shrinkage of the metaphosphate glasses were strongly composition dependent. Diversification of the components might help achieve higher  $\Delta S_{\text{mix}}$  glass systems with increased shrinkage. The underlying physical mechanism can be explained as follows. The increase in the types of alkali ions might potentially enhances  $\Delta S_{\text{mix}}$ , thus generating distinct inter-chain force. On one hand, the alkali metal ions with low field strength reduce inter-chain interaction, thus facilitating the micro-Brownian motion and the shrinkage of the stretched chains. On the other hand, alkali metal ions with high bond strength act as crosslinks among the chains. They can lock the relative position of the chains, thereby suppressing the macro-Brownian motion and allowing the chains to recover to their original states (Fig. 3a). Guided by this law, a high entropy glass system with the composition of 12.5Li<sub>2</sub>O-12.5Na<sub>2</sub>O-12.5K<sub>2</sub>O-12.5Cs<sub>2</sub>O-50P<sub>2</sub>O<sub>5</sub> was developed, and it exhibited the highest degree of entropic elasticity. This system features considerably long P-O-P chains and the best chain flexibility (Fig. 3b). Remarkably, the unprecedented properties such as extremely large elastic shrinkage (> 40%), notable anisotropy and non-Newtonian flow after loading (Fig. 3c), high

strength (> 1400 MPa), and improved Young's modulus (~148 GPa) (Fig. 3d) can be realized in metaphosphate glass fibers [80–82]. The above-mentioned results indicate that entropy engineering is an effective approach to tune the mechanical properties such as the entropic elasticity of glass and can even help to develop new highly elastic glasses.

#### 4.2. Electrical properties

The electrical properties such as electrical conductivity (opposite to resistivity) and dielectric loss of the material are strongly dependent on the mobility of charge carriers. For dielectric inorganic non-metallic glasses, the charge carriers are typically associated with relatively weakly bonded species, typically the monovalent alkali metal ions. The factors influencing the mobility of alkali ions may govern the electrical properties of such glasses.

Naturally, large ions are less mobile and thus exhibit lower electrical conductivity and dielectric loss compared to small ions. However, single alkali-containing glass systems can only display a limited tunable range of electrical conductivity and dielectric loss. In 1969, Isard et al. found that the mixed alkali effect, which was frequently observed in glass systems with relatively high  $\Delta S_{\text{mix}}$ , can be employed to effectively tune the electrical properties of the inorganic non-metallic glasses

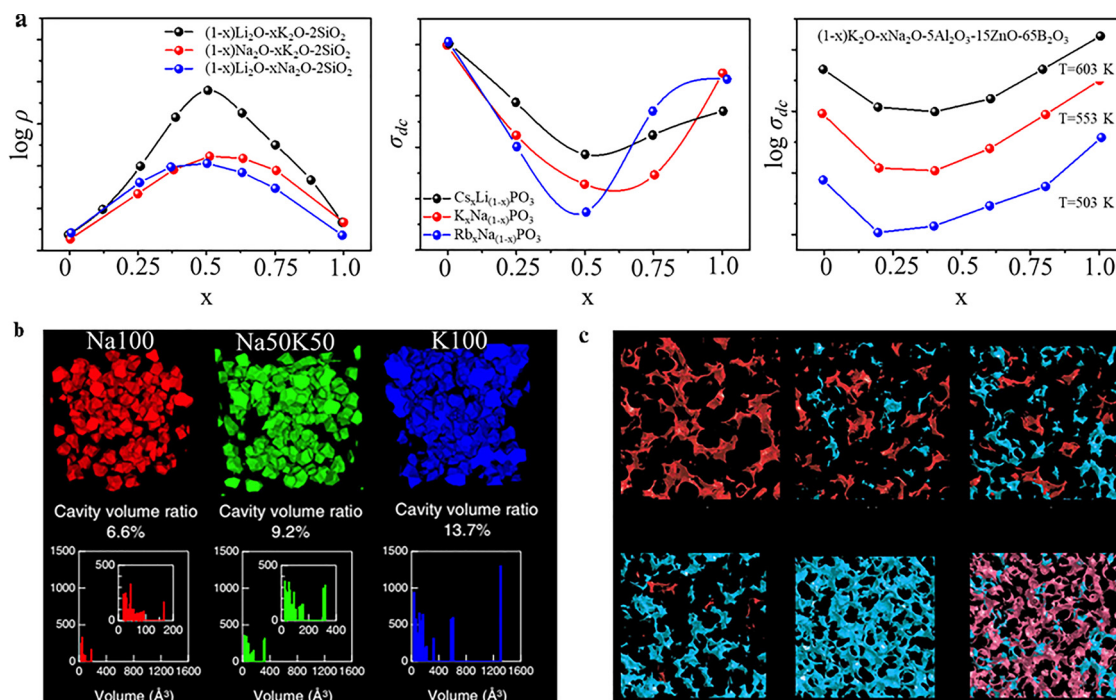


**Fig. 4. Entropy engineering for control of electrical properties of glass.** (a) Electrical conductivity ( $\sigma_{dc}$ ) or electrical resistivity ( $\rho$ ) as a function of alkali metal ion substitution ratio in silicate glass (left graph) [83]; phosphate glass (middle graph) [86]; and borate glass (right graph) [89]. (b) MD simulation on the cavity volume for the glass system of (mol%)22.7( $x\text{K}_2\text{O}-(1-x)\text{Na}_2\text{O}$ )-77.3 $\text{SiO}_2$  reported by Y. Onodera et al [93]. Upper panel: Visualization of cavities in alkali silicate glass with  $x = 0$  (left graph), 0.5 (middle graph) and 1.0 (right graph). Lower panel: Distribution of the cavities volume in alkali silicate glass with  $x = 0$  (left graph), 0.5 (middle graph) and 1.0 (right graph). (c) MD simulation on the conduction pathway for alkali ions in (mol%)50( $x\text{Li}_2\text{O}-(1-x)\text{Rb}_2\text{O}$ )-50 $\text{P}_2\text{O}_5$  glass system [94]. Upper panel: Conduction pathway for  $\text{Li}^+$  ions (blue) and  $\text{Rb}^+$  ions (red) with  $x = 0$  (left graph), 0.25 (middle graph) and 0.5 (right graph). Lower panel: Conduction pathway for  $\text{Li}^+$  ions (blue) and  $\text{Rb}^+$  ions (red) with  $x = 0.75$  (left graph) and 1.0 (middle graph); Blocked pathway (blue) and conduction pathway (pink) of  $\text{Li}^+$  in (mol%)25 $\text{Li}_2\text{O}$ -25 $\text{Rb}_2\text{O}$ -50 $\text{P}_2\text{O}_5$  glass system (right graph).

[83]. Interestingly, a gradual substitution of one type of alkali ion for other leads to a notable change of the electrical properties but in a nonlinear manner such that the overall ionic conductivity exhibits a pronounced minimum at approximately equimolar mixed alkali composition. Radiotracer studies show that the diffusivity of an alkali ion monotonically decreases as it is replaced by another alkali ion [84]. Taking 33.3 $\text{R}_2\text{O}$ -66.6 $\text{SiO}_2$  (mol%) glass system with  $R = (\text{Na}, \text{K})$  as an example, the electrical conductivity  $\sigma_{dc}$  of the mixed system 8.33 $\text{Na}_2\text{O}$ -24.98 $\text{K}_2\text{O}$ -66.6 $\text{SiO}_2$  (mol%) is superior to that of the subsystems, being ranked as 8.33 $\text{Na}_2\text{O}$ -24.98 $\text{K}_2\text{O}$ -66.6 $\text{SiO}_2 < 33.3\text{K}_2\text{O}$ -66.6 $\text{SiO}_2 < 33.3\text{Na}_2\text{O}$ -66.6 $\text{SiO}_2$  [83,85]. Significantly, this phenomenon has been demonstrated universally in a wide range of glass system such as  $\text{R}_2\text{O}$ - $\text{P}_2\text{O}_5$  [86] and  $\text{R}_2\text{O}$ - $\text{B}_2\text{O}_3$  [87–89] (Fig. 4a).

The atomistic mechanism of the observed phenomenon has been studied through structural characterizations and simulation, including neutron and X-ray diffractions, reverse Monte Carlo and molecular dynamics simulation [90–94]. It has been found that mixing of various types of alkali ions not only modifies the topological structure of glass matrix, but also changes the interaction among various alkali metal ions. The reverse Monte Carlo and molecular dynamics (MD) simulations show that alkali metal ions are distributed in the “channels” of structural network, i.e., alkali metal ions can only migrate through extremely narrow pathway. Mixed-alkali system exhibits smaller maximum cavity size compared with that in the single alkali system. As a result, the movement of the large alkali metal ion would be significantly suppressed by the narrow channel of the high entropy mixed alkali system, which is named as the bottleneck effect [93] (Fig. 4b). The notable energy mismatch among different alkali metal ion sites and the low dimensionality of the migration pathway cooperatively reduces the ionic jumping probability. Thus, the migration pathways of small alkali metal ions would be partially blocked by the larger ones [94] (Fig. 4c). These factors can be discerned directly by measuring the diffusion of a third al-

kali ion (Rb) as trace impurity in a binary mixed alkali (Na-Cs trisilicate) glass series [95]. These two factors (i.e., the bottleneck effect and the reduced ionic jumping probability) contribute to the decrease of electrical conductivity and dielectric loss in the mixed alkali oxide glasses. The above-mentioned mechanism can also be defined as “sluggish kinetics”, which has been widely recognized as a prominent effect in high entropy alloys and ceramics. Further, pairing of alkali ions is considered important for the migration of alkali ions, and pairing of unlike ions would be preferred from the perspective of entropy of mixing. Thus, it is expected that the entropy engineered glass system such as the triple or quadruple mixed alkali glass systems may display superior electrical properties.

#### 4.3. Chemical durability

There are several factors, such as the compactness of glass network and mobility of the network modifier cations, which may affect the chemical durability of inorganic non-metallic glasses. In addition to the electrical properties, the chemical durability of inorganic non-metallic glasses is also associated with the mixed alkali effect, which can reduce the mobility of alkali ions. For example, the hydrolysis of alkali-containing oxide glasses mainly results from the ion exchange between protons from the environment and alkali metal ions from glass. Thus, the chemical durability, especially hydrolytic resistance of oxide glasses is related to the mobility of the alkali metal ions. Like the sluggish kinetics effect of high entropy ceramics and alloys, the mixed alkali systems should exhibit lower mobility of alkali metal ions, and thus an improved chemical durability can be expected [96] (Fig. 5a, b). This improvement has been confirmed by a series of experiments [85, 97–99] (Fig. 5c). Therefore, it can be anticipated that the entropy engineering via diversification of the alkali ions can be employed to engineer the chemical durability of the mixed alkali inorganic non-metallic



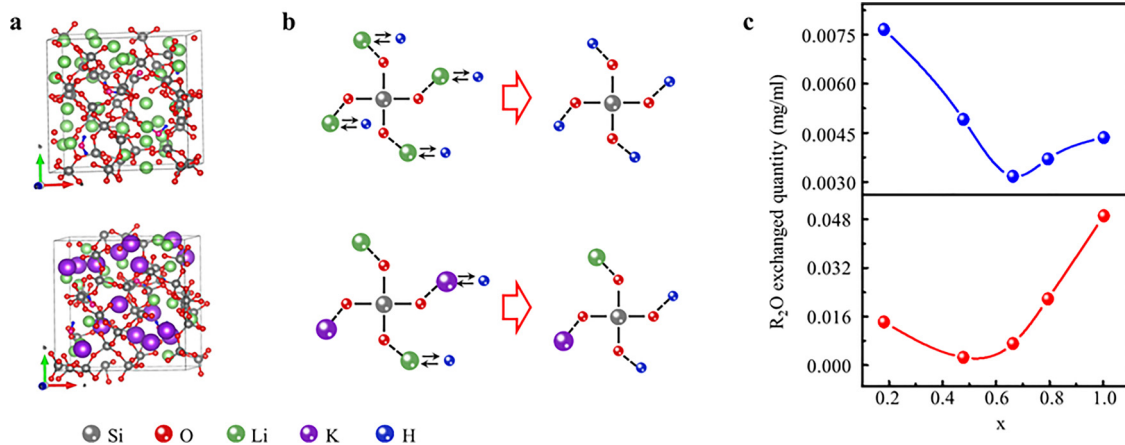


**Fig. 5. Entropy engineering for control of chemical durability of glass.** (a) Topological structures of Li<sub>2</sub>O-SiO<sub>2</sub> glass and Li<sub>2</sub>O-K<sub>2</sub>O-SiO<sub>2</sub> glass [96]. (b) Schematic illustration of hydrolysis of single and mixed alkali silicate glass. (c) Composition dependent alkali metal ions exchanged quantity for (mol%)17(xK<sub>2</sub>O-(1-x)Na<sub>2</sub>O)-10CaO-73SiO<sub>2</sub> (red) and (mol%)16(xK<sub>2</sub>O-(1-x)Na<sub>2</sub>O)-10CaO-74SiO<sub>2</sub> (blue). The glass samples are immersed in HCl solutions [85].

glasses, pointing to various promising applications such as hydrolytic resistant bioactive glasses, protection cover, and on-chip chemical reactor [100].

#### 4.4. Optical properties

The optical properties of glass are crucial for various applications such as optical imaging, optical communication, and laser. Glass bulk and fibers can be activated with rare-earth or transition-metal or main-group ions via incorporation of active dopants into glass matrix. In this case, the optical properties are governed by both the chemical state and the chemical environment of dopants. It is necessary to note that diversification of component elements of the system also affects the chemical state and their chemical environment of dopants, thus resulting in diverse optical properties of inorganic non-metallic glasses [101–103]. The approach of components diversification, frequently employed in entropy engineering, to enhance the optical performances of inorganic non-metallic glasses, can be described through the following two considerations.

##### 4.4.1. Tuning the aggregation process of dopants

Modifying  $S_{\text{conf}}$  through multicomponent diversification can help adjust the aggregation process of the atoms or ions by so-called entropy-stabilized effect for alloys and ceramics. Like that of the alloys and ceramics, the strategy might be also suitable for tuning the aggregation of dopants in inorganic non-metallic glasses. To illustrate, consider the development of high average power laser glasses doped with various rare-earth active dopants as a typical example. In 1986, Arai first studied the clustering of Nd<sup>3+</sup> dopants in pure silica glass that is composed of [SiO<sub>4</sub>] structural units. It was found that Nd<sup>3+</sup> dopants cannot be well incorporated into the rigid [SiO<sub>4</sub>] network, leading to the unwanted dopant aggregation and phase separation, and hence, the extremely poor lasing performance [104]. Furthermore, diversifying the composition with Al<sub>2</sub>O<sub>3</sub> and P<sub>2</sub>O<sub>5</sub> allows to effectively prevent the unexpected Nd<sup>3+</sup> aggregation, and thereby to improve the luminescent properties [102,103]. Monteil et al [105], found that co-doping with Al may lead to a change of the local distribution of Eu<sup>3+</sup> dopants (Fig. 6a). Funabiki et al [106], proposed that the co-doped P and Al played two different roles. The role of P is associated with the formation of a unique solvation shell, while the role of Al is directly related to the entropy driven suppression of phase-separation (Fig. 6a). The exact roles of P and Al are still not fully clarified. Nevertheless, some possible explanations can be given as follows. The addition of Al<sub>2</sub>O<sub>3</sub> and P<sub>2</sub>O<sub>5</sub> would not only increase the number of the components, but also diversify the microstructures. Especially, various types of structural units including

[AlO<sub>4</sub>], [AlO<sub>6</sub>], [PO<sub>4</sub>] and [PO<sub>5</sub>] are presented in the structural network, and therefore the  $S_{\text{conf}}$  ( $\Delta S_{\text{mix}} > 0$ ) of the system could be higher than that of the system with fewer structural units. Consequently, the relative high entropy prevents the clustering of rare-earth dopants and thereby improve the optical performance of the glass, which is similar to the entropy-stabilized effect in alloys and ceramics. In addition to rare-earth metal dopants, main-group (e.g., Bi) [107] and noble metal dopants (e.g., Au and Ag) were also frequently employed in active photonics [108]. Interestingly, various kinds of the aggregation centers, such as Bi<sup>+</sup>, Bi<sub>5</sub><sup>3+</sup>, Bi nanoparticles, and Ag<sup>+</sup>, Ag<sub>2</sub><sup>+</sup>, Ag nanoparticles can be stabilized in multicomponent glass systems (Fig. 6b). In a striking case, the chemical states of various dopants can be precisely tuned by changing the topological structure of glass, leading to intriguing tunable and ultra-broadband luminescence (Fig. 6b). Although the detailed tuning mechanism still needs to be revealed, it is supposed that the entropy evolution of the systems would be a contributing factor.

##### 4.4.2. Adjusting chemical environment around the dopants

Entropy engineering strategy also enables the adjustment of the local chemical environment around the dopants. As analyzed above, high entropy systems possess extremely rich local configurations, and this is highly favorable for inhomogeneous broadening. This may lead to the extension or shift of the optical spectrum of the glass, which has strong impact on optical performances, such as broadband optical amplification, tunable lasing and ultra-short pulse generation. The contribution of multiple configurations to the inhomogeneous broadening can be supported by experimental evidence. One typical example is the spectral broadening of Er<sup>3+</sup>-doped multicomponent tellurite glass (10Na<sub>2</sub>O-10ZnO-80TeO<sub>2</sub> in mol%) [109,110]. The structural analysis indicates that Te-O can form various unique configuration units such as [TeO<sub>4</sub>], [TeO<sub>3</sub>] and [TeO<sub>3+1</sub>] in glass systems (Fig. 6c). Thus, the tellurite glass system can be considered as a typical high entropy system. As a result, broadband emission from Er<sup>3+</sup> dopant with the bandwidth of more than ~50 nm can be observed in this system. This is in strong contrast to the case of Er<sup>3+</sup>-doped silica glass which only exhibits narrow emission with the bandwidth of ~8 nm (Fig. 6c). Another effective way to diversify the configurations of the system for inhomogeneous broadening is the direct diversification of glass network formers [111–115]. For example, the Bi-doped hybrid germanium silicate glass (79.5GeO<sub>2</sub>-17SiO<sub>2</sub>-3Al<sub>2</sub>O<sub>3</sub> in mol%) exhibits broadband and flat emission feature compared with the pure germanate glass system (96.5GeO<sub>2</sub>-3Al<sub>2</sub>O<sub>3</sub> in mol%). The Er-doped hybrid glass fiber shows broader optical amplification compared with the silica fiber, and even supports laser operation beyond 1630 nm [116]. In addition, in the Ni<sup>2+</sup>-doped system with ternary network formers (25.53Li<sub>2</sub>O-21.53Ta<sub>2</sub>O<sub>5</sub>-35.29SiO<sub>2</sub>-17.65Al<sub>2</sub>O<sub>3</sub> in mol%), unusual



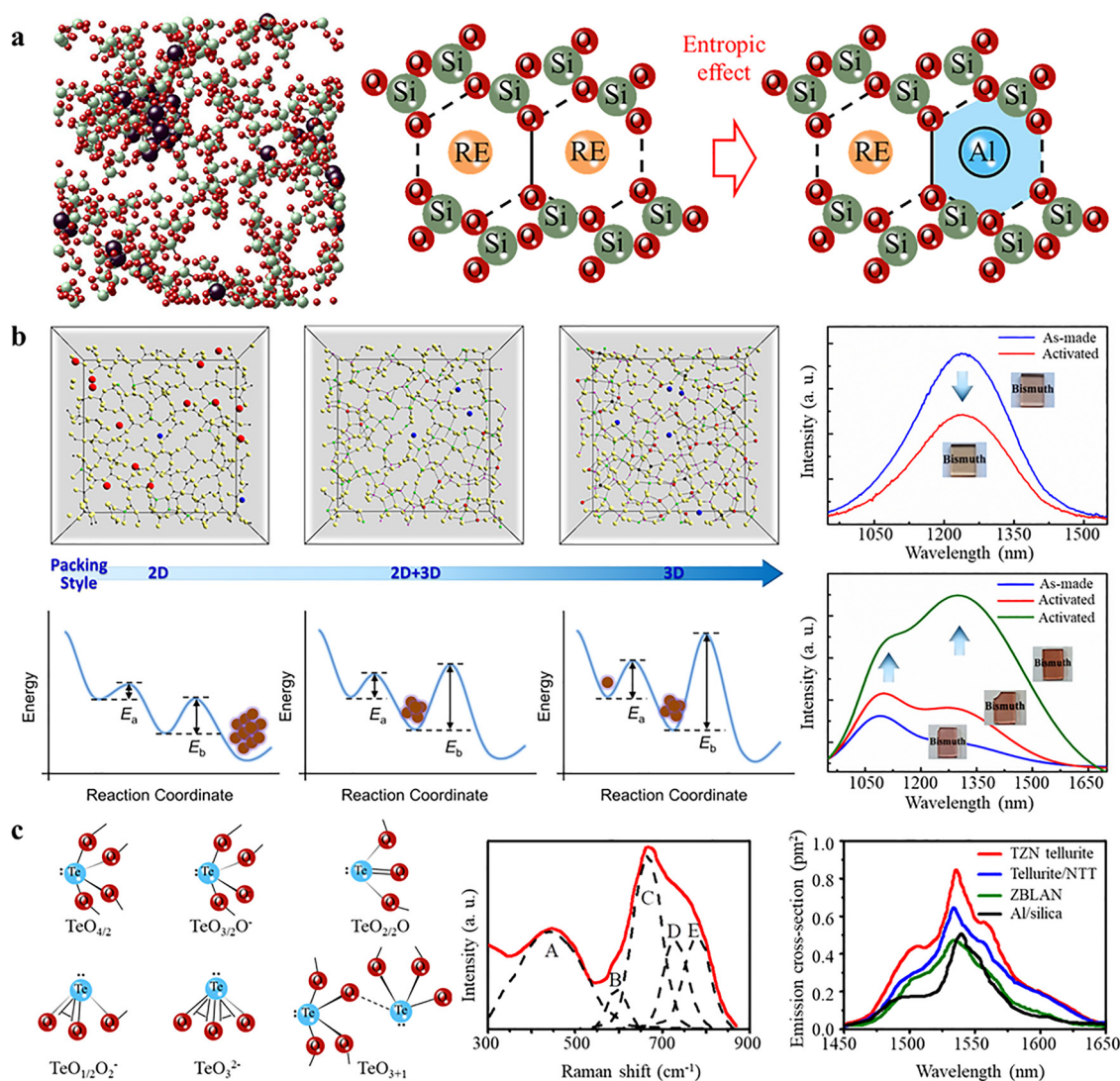


**Fig. 6.** Entropy engineering for control of optical properties of glass. (a) MD simulation and schematic illustration of the entropic control to avoid the aggregation of rare-earth dopants in glass matrix [105]. (b) Topological engineering for tuning the chemical state of main group dopants in glass. Left: MD simulation and schematic illustration on the topological structure dependent chemical state of dopant in distinct multicomponent glass system, with O atoms colored yellow, B atoms colored black, Si atoms colored pink, Al colored green, Bi colored blue, alkaline-earth atoms colored red. Right: The topological structure dependent near-infrared luminescence change from bismuth dopant [107]. (c) Left: The local structures of various  $[\text{TeO}_n]$  polyhedrons. Middle: Raman spectrum of a typical multicomponent tellurite glass [109]. Right: Comparison of the near-infrared luminescence of  $\text{Er}^{3+}$  dopant in various multicomponent glass systems with that in silica glass [110].

inhomogeneous broadening with flat emission ( $\sim 480$  nm) has been observed after nanocrystallization [117]. To clarify the origin of this phenomenon, Zhou et al. employed high-angle annular dark-field scanning transmission electron microscopy to explore the microstructure of the above glass. They directly observed the mesoscale chemical heterogeneities, which were similar to the pronounced composition fluctuations in high entropy alloy composed of  $\text{CrFeCoNiPd}$  [118]. They argued that this heterogeneity could genetically dominate the spectral features of the glass. These results imply opportunity and feasibility to develop the next-generation broadband photonic devices with significant applications in high-capacity telecommunication, remote sensing and defense.

## 5. Summary and outlook

The entropy engineering is an effective way not only for tuning the glass forming ability, but also for controlling the mechanical, electrical as well as optical properties of inorganic non-metallic glasses. Thus, this new strategy can be valuable for developing novel functional in-

organic non-metallic glass materials. However, there remain challenges as well as opportunities for applying the entropy engineering concept in developing advanced functional inorganic non-metallic glasses. We have pointed out four potential research directions related to entropy engineering.

### 5.1. Entropy calculation for inorganic non-metallic glass

$S_{\text{conf}}$  can be calculated based on local configuration statistics and thermal measurement, which are used for both the Boltzmann entropy and the Clausius entropy, respectively. The Boltzmann entropy calculation is usually limited to alloy and ceramic materials, and is not suitable for inorganic non-metallic glasses owing to their complex local structure. MD simulation can provide valuable information on the Boltzmann entropy calculation. For example, MD simulation has been recently conducted in reconstructing microstructures of inorganic non-metallic glasses, and the local configuration statistics can be potentially achieved. Despite some progress, there is still plenty of room for this strategy to be implemented. The main challenge for MD into quantify

the Boltzmann entropy is to reveal the exact structures of inorganic non-metallic glass, since the non-crystalline solids are rather complicated, and the theoretical simulation can be time-consuming. In any case, the Clausius entropy calculation based on experimental thermal analysis for inorganic non-metallic glasses can be performed to verify and modify the Boltzmann entropy obtained via MD calculations. The challenge for the Clausius entropy calculation is associated with the lack of thermodynamic data, especially the heat capacities of glass, super-cooled liquid, and equilibrium liquid at various temperatures. Thus, precise entropy calculation for inorganic non-metallic glasses is strongly dependent on the future development of computational materials science and the expansion of thermodynamic database.

### 5.2. Investigation of the influence of entropy on glass stability

Understanding the influence of entropy and enthalpy on glass stability, such as the glass formation, phase separation, clustering behavior and homogeneity is critical for glass design based on the entropy engineering strategy. Unfortunately, the existing models are insufficient for quantitatively describing these effects. A combined method based on both the MD and the first-principle simulation may be useful for exploring the relation between local structure and entropy at given temperatures, leading to the establishment of a precise model. This model should enable the redefinition of the contribution of entropy in both thermodynamics and kinetics processes for glass stability and give a better understanding of the separated influence of entropy and enthalpy on glass stability. Once this type of model is created, the giant expansion of the database of high entropy glass system can be expected.

### 5.3. New techniques for tuning entropy of inorganic non-metallic glasses

Developing high configurational entropy materials relies on the available methods to increase the entropy of the system. The classic way is the rational diversification of the component elements. In addition, as a unique feature in glass, cooling process plays a critical role in freezing various configurations of the structural units ( $\Delta S'_{\text{conf}}$  design). It can be expected that faster cooling rate potentially allows obtaining higher  $S_{\text{conf}}$  ( $\Delta S'_{\text{conf}} > 0$ ). Thus, a rational control of cooling rate is supposed to be an effective approach for adjusting  $S_{\text{conf}}$  in glass. It is believed that development of new fabrication techniques would be a promising way to raise  $S_{\text{conf}}$  of inorganic non-metallic glasses.

### 5.4. Development of advanced inorganic non-metallic glasses based on entropy engineering strategy

Entropy engineering is expected to enable the rational and efficient development of advanced functional inorganic non-metallic glasses. The current progress is mainly limited to the multicomponent oxide glasses, and it is critically important to expand the category of the glass systems. More specifically, the entropy-property relation in other special glass systems such as fluoride, chalcogenide and hybrid glasses should be explored. It can be envisioned that a series of advanced inorganic non-metallic glasses with greatly enhanced mechanical, electrical, chemical, and optical properties can be developed by utilizing the entropy engineering strategy. These entropy-engineered glass materials are supposed to be the next-generation candidates for various fundamental applications. Entropy engineering for inorganic non-metallic glasses has just been in infancy and needs to be intensively tested for a large range of inorganic non-metallic glass systems. At this initial stage it would appear prudent, it is significant to begin the research from the low entropy systems with simple composition and then expand it to the complex higher entropy candidates.

### Declaration of Competing Interest

The authors declare that they have no conflicts of interest in this work.

### Acknowledgments

The authors gratefully acknowledge financial support from the National Key Research and Development Program of China (Grant No. 2020YFB1805901), the National Science Fund for Distinguished Young Scholars (Grant No. 62125502), the National Natural Science Foundation of China (Grant No. 51972113), the Key Program of Guangzhou Scientific Research Special Project (Grant No. 201904020013), the Key Research and Development Program of Guangzhou (Grant No. 202007020003), the Science and Technology Project of Guangdong Province (Grant No. 2021A0505030004), the Local Innovative and Research Teams Project of Guangdong Pearl River Talents Program (Grant No. 2017BT01 × 137), and the Fundamental Research Funds for the Central University.

### References

- [1] J.W. Yeh, S.J. Lin, S.K. Chen, et al., Nanostructured high-entropy alloys with multiple principal elements: novel alloy design concepts and outcomes, *Adv. Eng. Mater.* 6 (2004) 299.
- [2] B. Cantor, I.T.H. Chang, P. Knight, et al., Microstructural development in equiatomic multicomponent alloys, *Mater. Sci. Eng. A* 375–377 (2004) 213.
- [3] M.R. Chen, S.J. Lin, J.W. Yeh, et al., Microstructure and properties of  $\text{Al}_{0.5}\text{CoCrCuFeNiTi}_x$  ( $x=0-2.0$ ) high-entropy alloys, *Mater. Trans.* 47 (2006) 13951401.
- [4] Y.F. Kao, T.J. Chen, S.K. Chen, et al., Microstructure and mechanical property of as-cast, -homogenized, and -deformed  $\text{Al}_x\text{CoCrFeNi}$  ( $0 \leq x \leq 2$ ) high-entropy alloys, *J. Alloy. Compd.* 488 (2009) 57.
- [5] C. Ng, S. Guo, J. Luan, et al., Phase stability and tensile properties of Co-free  $\text{Al}_{0.5}\text{CoCrCuFeNi}_2$  high-entropy alloy, *J. Alloy. Compd.* 584 (2014) 530.
- [6] Z. Wu, H. Bei, F. Otto, et al., Recovery, recrystallization, grain growth and phase stability of a family of FCC-structured multi-component equiatomic solid solution alloys, *Intermetallics* 46 (2014) 131.
- [7] M.R. Chen, S.J. Lin, J.W. Yeh, et al., Effect of vanadium addition on the microstructure, hardness, and wear resistance of  $\text{Al}_{0.5}\text{CoCrCuFeNi}$  high-entropy alloy, *Metall. Mater. Trans.* 37 (2006) 1363.
- [8] S. Guo, C. Ng, C.T. Liu, Anomalous solidification microstructures in Co-free  $\text{Al}_x\text{CoCrCuFeNi}_2$  high-entropy alloys, *J. Alloy Compd.* 557 (2013) 77.
- [9] O.N. Senkov, G.B. Wilks, J.M. Scott, et al., Mechanical properties of  $\text{Nb}_{25}\text{Mo}_{25}\text{Ta}_{25}\text{W}_{25}$  and  $\text{V}_{20}\text{Nb}_{20}\text{Mo}_{20}\text{Ta}_{20}\text{W}_{20}$  refractory high entropy alloys, *Intermetallics* 19 (2011) 698.
- [10] O.N. Senkov, G.B. Wilks, D.B. Miracle, et al., Refractory high-entropy alloys, *Intermetallics* 18 (2010) 1758.
- [11] X. Yang, Y. Zhang, P.K. Liaw, Microstructure and compressive properties of  $\text{NbTiVTaAl}_x$  high entropy alloys, *Proc. Eng.* 36 (2012) 292.
- [12] K.M. Youssef, A.J. Zaddah, C. Niu, et al., A novel low-density, high-hardness, high-entropy alloy with close-packed single-phase nanocrystalline structures, *Mater. Res. Lett.* 3 (2015) 95.
- [13] A. Takeuchi, K. Amiya, T. Wada, et al., High-entropy alloys with a hexagonal close-packed structure designed by equi-atomic alloy strategy and binary phase diagrams, *JOM* 66 (2014) 1984.
- [14] M. Feuerbacher, M. Heidelmann, C. Thomas, Hexagonal high-entropy alloys, *Mater. Res. Lett.* 3 (2015) 1.
- [15] Y.F. Ye, Q. Wang, J. Lu, et al., High-entropy alloy: challenges and prospects, *Mater. Today* 19 (2016) 349.
- [16] R. Wei, J. Tao, H. Sun, et al., Soft magnetic  $\text{Fe}_{26.7}\text{Co}_{26.7}\text{Ni}_{26.6}\text{Si}_9\text{B}_{11}$  high entropy metallic glass with good bending ductility, *Mater. Lett.* 197 (2017) 87.
- [17] Y. Tong, J.C. Qiao, C. Zhang, et al., Mechanical properties of  $\text{Ti}_{16.7}\text{Zr}_{16.7}\text{Hf}_{16.7}\text{Cu}_{16.7}\text{Ni}_{16.7}\text{Be}_{16.7}$  high-entropy bulk metallic glass, *J. Non-Cryst. Solids* 452 (2016) 57.
- [18] X.Y. Wang, W.L. Dai, M. Zhang, et al., Thermoplastic micro-formability of  $\text{TiZrHfNiCuBe}$  high entropy metallic glass, *J. Mater. Sci. Technol.* 34 (2018) 40.
- [19] H.Y. Ding, K.F. Yao, High entropy  $\text{Ti}_{20}\text{Zr}_{20}\text{Cu}_{20}\text{Ni}_{20}\text{Be}_{20}$  bulk metallic glass, *J. Non-Cryst. Solids* 364 (2013) 9.
- [20] H.Y. Ding, Y. Shao, P. Gong, et al., A senary  $\text{TiZrHfCuNiBe}$  high entropy bulk metallic glass with large glass-forming ability, *Mater. Lett.* 125 (2014) 151.
- [21] X.Z. Gao, Y.P. Lu, B. Zhang, et al., Microstructural origins of high strength and high ductility in an  $\text{AlCoCrFeNi}_{2.1}$  eutectic high-entropy alloy, *Acta Mater.* 141 (2017) 59.
- [22] C.P. Lee, Y.Y. Chen, C.Y. Hsu, et al., The effect of boron on the corrosion resistance of the high entropy alloys  $\text{Al}_{0.5}\text{CoCrCuFeNiB}_x$ , *J. Electrochem. Soc.* 154 (2007) C424.
- [23] B. Gludovatz, A. Hohenwarter, D. Catoor, et al., A fracture-resistant high-entropy alloy for cryogenic applications, *Science* 345 (2014) 1153.
- [24] H. Zhang, Y.Z. He, Y. Pan, Enhanced hardness and fracture toughness of the laser-solidified  $\text{FeCoNiCrCuTiMoAlSiB}_{0.5}$  high-entropy alloy by martensite strengthening, *Scripta Mater.* 69 (2013) 342.
- [25] W.D. Li, P.K. Liaw, Y.F. Gao, et al., Fracture resistance of high entropy alloys: a review, *Intermetallics* 99 (2018) 69.
- [26] C. Oses, C. Toher, S. Curtarolo, High-entropy ceramics, *Nat. Rev. Mater.* 5 (2020) 295.

- [27] C.M. Rost, E. Sachet, T. Borman, et al., Entropy-stabilized oxides, *Nat. Commun.* 6 (2005) 8485.
- [28] A.Q. Mao, H.Z. Xiang, Z.G. Zhang, et al., Solution combustion synthesis and magnetic property of rock-salt  $(\text{Co}_{0.2}\text{Cu}_{0.2}\text{Mg}_{0.2}\text{Ni}_{0.2}\text{Zn}_{0.2})\text{O}$  high-entropy oxide nanocrystalline powder, *J. Magn. Magn. Mater.* 484 (2019) 245.
- [29] J. Dąbrowa, M. Stygar, A. Mikula, et al., Synthesis and microstructure of the  $(\text{Co}, \text{Cr}, \text{Fe}, \text{Mn}, \text{Ni})_2\text{O}_4$  high entropy oxide characterized by spinel structure, *Mater. Lett.* 216 (2018) 32.
- [30] K.P. Tseng, Q. Yang, S.J. McCormack, et al., High-entropy, phase-constrained, lanthanide sesquioxide, *J. Am. Ceram. Soc.* 103 (2019) 569.
- [31] A.Q. Mao, H.Z. Xiang, Z.G. Zhang, et al., A new class of spinel high-entropy oxides with controllable magnetic properties, *J. Magn. Magn. Mater.* 497 (2020) 165884.
- [32] E. Castle, T. Csanádi, S. Grasso, et al., Processing and properties of high-entropy ultra-high temperature carbides, *Sci. Rep.* 8 (2018) 8609.
- [33] P. Sarker, T. Harrington, C. Toher, et al., High-entropy high-hardness metal carbides discovered by entropy descriptors, *Nat. Commun.* 9 (2018) 4980.
- [34] B.L. Ye, T.Q. Wen, K.H. Wang, et al., First-principles study, fabrication, and characterization of  $(\text{Hf}_{0.2}\text{Zr}_{0.2}\text{Ta}_{0.2}\text{Nb}_{0.2}\text{Ti}_{0.2})\text{C}$  high-entropy ceramic, *J. Am. Ceram. Soc.* 102 (2019) 4344.
- [35] T.J. Harrington, J. Gild, P. Sarker, et al., Phase stability and mechanical properties of novel high entropy transition metal carbides, *Acta Mater.* 166 (2019) 271.
- [36] D. Liu, H.H. Liu, S.S. Ning, et al., Synthesis of high-purity high-entropy metal diboride powders by boro/carbothermal reduction, *J. Am. Ceram. Soc.* 102 (2019) 7071.
- [37] P.H. Mayrhofer, A. Kirnbauer, Ph. Ertelthaler, et al., High-entropy ceramic thin films: a case study on transition metal diborides, *Scripta Mater.* 149 (2018) 93.
- [38] J. Gild, Y.Y. Zhang, T. Harrington, et al., High-entropy metal diborides: a new class of high-entropy materials and a new type of ultrahigh temperature ceramics, *Sci. Rep.* 6 (2016) 37946.
- [39] D. Liu, T.Q. Wen, B.L. Ye, et al., Synthesis of superfine high-entropy metal diboride powders, *Scripta Mater.* 167 (2019) 110.
- [40] J. Gild, J. Braun, K. Kaufmann, et al., A high-entropy silicide:  $(\text{Mo}_{0.2}\text{Nb}_{0.2}\text{Ta}_{0.2}\text{Ti}_{0.2}\text{W}_{0.2})\text{Si}_2$ , *J. Mater. Sci.* 5 (2019) 337.
- [41] Y. Qin, J.X. Liu, F. Li, et al., A high entropy silicide by reactive spark plasma sintering, *J. Adv. Ceram.* 8 (2019) 148.
- [42] Y. Zhang, W.M. Guo, Z.B. Jiang, Q.Q. Zhu, et al., Dense high-entropy boride ceramics with ultra-high hardness, *Scripta Mater.* 164 (2019) 135.
- [43] P. Malinowski, S. Fritze, L. Riekehr, et al., Synthesis and characterization of multicomponent  $(\text{CrNbTaTiW})\text{C}$  films for increased hardness and corrosion resistance, *Mater. Design* 149 (2018) 59.
- [44] M. Dinu, I. Pana, V. Braic, et al., In vitro corrosion resistance of Si containing multi-principal element carbide coatings, *Mater. Corros.* 67 (2016) 908.
- [45] X.L. Yan, L. Constantin, Y.F. Lu, et al.,  $(\text{Hf}_{0.2}\text{Zr}_{0.2}\text{Ta}_{0.2}\text{Nb}_{0.2}\text{Ti}_{0.2})\text{C}$  high-Entropy ceramics with low thermal conductivity, *J. Am. Ceram. Soc.* 101 (2018) 4486.
- [46] Z.F. Zhao, H.M. Xiang, F.Z. Dai, et al.,  $(\text{La}_{0.2}\text{Ce}_{0.2}\text{Nd}_{0.2}\text{Sm}_{0.2}\text{Eu}_{0.2})\text{Zr}_2\text{O}_7$ : a novel high-entropy ceramic with low thermal conductivity and sluggish grain growth rate, *J. Mater. Sci. Technol.* 35 (2019) 2647.
- [47] M. Moesgaard, R. Keding, J. Skibsted, et al., Evidence of intermediate-range order heterogeneity in calcium aluminosilicate glasses, *Chem. Mater.* 22 (2010) 4471.
- [48] Y.Z. Yue, The iso-structural viscosity, configurational entropy and fragility of oxide liquids, *J. Non-Cryst. Solids* 355 (2009) 737.
- [49] J.C. Mauro, Y.Z. Yue, A.J. Ellison, et al., Viscosity of glass-forming liquids, *P. Natl. Acad. Sci. USA* 106 (2009) 19780.
- [50] G.P. Johari, et al., Decrease in the configurational and vibrational entropies on supercooling a liquid and their relations with the excess entropy, *J. Non-Cryst. Solids* 307 (2002) 387.
- [51] T.Q. Wen, H.H. Liu, B.L. Ye, et al., High-entropy aluminosilicates: a novel class of high-entropy ceramics, *Sci. China Mater.* 63 (2020) 300.
- [52] Q.J. Zheng, Y.F. Zhang, M. Montazerian, et al., Understanding glass through differential scanning calorimetry, *Chem. Rev.* 119 (2020) 7874.
- [53] A. Takada, R. Conradt, P. Richet, Residual entropy and structural disorder in glass: a two-level model and a review of spatial and ensemble vs. temporal sampling, *J. Non-cryst. Solids* 360 (2013) 13.
- [54] R. Conradt, Chemical structure, medium range order, and crystalline reference state of multicomponent oxide liquids and glasses, *J. Non-cryst. Solids* 345–346 (2004) 16.
- [55] U. Fotheringham, A. Baltes, R. Müller, et al., The residual configurational entropy below the glass transition: determination for two commercial optical glasses, *J. Non-cryst. Solids* 355 (2009) 642.
- [56] A. Takada, R. Conradt, P. Richet, Residual entropy and structural disorder in glass: a review of history and an attempt to resolve two apparently conflicting views, *J. Non-cryst. Solids* 429 (2015) 33.
- [57] P. Richet, Viscosity and configurational entropy of silicate melts, *Geochim. Cosmochim. Acta* 48 (1983) 471.
- [58] P. Richet, R.A. Robie, B.S. Hemingway, et al., Entropy and structure of silicate glasses and melts, *Geochim. Cosmochim. Acta* 57 (1992) 2751.
- [59] B.J. Speedy, The entropy of a glass, *Mol. Phys.* 80 (1993) 1105.
- [60] G. Adam, J.H. Gibbs, On the temperature dependence of cooperative relaxation properties in glass-forming liquids, *J. Chem. Phys.* 43 (1965) 139.
- [61] Y.Z. Yue, S.L. Jensen, J.C. Christiansen, Determination of the fictive temperature for a hyperquenched glass, *Chem. Phys. Lett.* 357 (2002) 20.
- [62] L. Hornbøll, Y.Z. Yue, et al., Enthalpy relaxation in hyperquenched glasses of different fragility, *J. Non-Cryst. Solids* 354 (2007) 1862.
- [63] Y.F. Zhang, L.N. Hu, S.J. Liu, et al., Sub- $T_g$  enthalpy relaxation in an extremely unstable oxide glass and its implication for structural heterogeneity, *J. Non-Cryst. Solids* 381 (2013) 23.
- [64] J.R. Zhang, X.Y. Zhang, Y. Li, et al., High-entropy oxides  $10\text{La}_2\text{O}_3\text{-}20\text{TiO}_2\text{-}10\text{Nb}_2\text{O}_5\text{-}20\text{WO}_3\text{-}20\text{ZrO}_2$  amorphous spheres prepared by containerless solidification, *Mater. Lett.* 244 (2019) 167.
- [65] A. Sarkar, R. Djenadic, D. Wang, et al., Rare earth and transition metal based entropy stabilised perovskite type oxides, *J. Eur. Ceram. Soc.* 38 (2018) 2318.
- [66] X.F. Liu, J.J. Zhou, S.F. Zhou, et al., Transparent glass-ceramics functionalized by dispersed crystals, *Prog. Mater. Sci.* 97 (2018) 38.
- [67] K. Meyer, *Physikalisch-Chemische Kristallographie*, Dt Verlag für Grundstoffindustrie, Leipzig, 1968.
- [68] W.D. Kingery, et al., *Uhlmann DR. Introduction to Ceramics*, John Wiley & Sons, New York, 1976.
- [69] R.X. Li, Y. Zhang, Entropy and glass formation, *Acta Phys. Sin.* 66 (2017) 177101.
- [70] A.L. Greer, Confusion by design, *Nature* 366 (1993) 303.
- [71] H. Lin, S.B. Jiang, J.F. Wu, et al.,  $\text{Er}^{3+}$  doped  $\text{Na}_2\text{O-Nb}_2\text{O}_5\text{-TeO}_2$  glasses for optical waveguide laser and amplifier, *J. Phys. D: Appl. Phys.* 36 (2003) 812.
- [72] R.T. Hart, J.W. Zwaninger, P.L. Lee, The crystalline phase of  $(\text{K}_2\text{O})_{15}(\text{Nb}_2\text{O}_5)_{15}(\text{TeO}_2)_{70}$  glass ceramic is a polymorph of  $\text{K}_2\text{Te}_4\text{O}_9$ , *J. Non-Cryst. Solids* 337 (2004) 48.
- [73] S. Blanchandin, P. Thomas, P. Marchet, et al., New heavy metal oxide glasses: investigations within the  $\text{TeO}_2\text{-Nb}_2\text{O}_5\text{-Bi}_2\text{O}_3$  system, *J. Alloy. Compd.* 347 (2002) 206.
- [74] J. Kjeldsen, A.C. Rodrigues, S. Mossin, et al., Critical  $\text{V}_2\text{O}_5/\text{TeO}_2$  ratio inducing abrupt property changes in vanadium tellurite glasses, *J. Phys. Chem. B* 118 (2014) 14942.
- [75] Y.F. Zhang, P.X. Wang, T. Zheng, et al., Enhancing Li-ion battery anode performances via disorder/order engineering, *Nano Energy* 49 (2018) 596.
- [76] T.F. Soules, A molecular dynamic calculation of the structure of  $\text{B}_2\text{O}_3$  glass, *J. Chem. Phys.* 73 (1980) 4032.
- [77] K. Januchta, T. To, M.S. Bødker, et al., Elasticity, hardness, and fracture toughness of sodium aluminoborosilicate glasses, *J. Am. Ceram. Soc.* 102 (2019) 4520.
- [78] W. Soppe, C. van der Marel, W.F. van Gunsteren, et al., New insights into the structure of  $\text{B}_2\text{O}_3$  glass, *J. Non-Cryst. Solids* 103 (1988) 201.
- [79] R.K. Brow, Review: the structure of simple phosphate glasses, *J. Non-Cryst. Solids* 263–264 (2000) 1.
- [80] S. Inaba, H. Hosono, S. Ito, Entropic shrinkage of an oxide glass, *Nat. Mater.* 14 (2015) 312.
- [81] J. Endo, S. Inaba, S. Ito, Mechanical properties of anisotropic metaphosphate glass, *J. Am. Ceram. Soc.* 98 (2015) 2767.
- [82] M. Braun, Y.Z. Yue, C. Rüsel, C. Jäger, Two-dimensional nuclear magnetic resonance evidence for structural orientation in extruded phosphate glass, *J. Non-Cryst. Solids* 241 (1998) 204.
- [83] J.O. Isard, The mixed alkali effect in glass, *J. Non-Cryst. Solids* 1 (1969) 235.
- [84] H. Jain, N.L. Peterson, H.L. Dowling, Tracer Diffusion and electrical conductivity in sodium-cesium silicate glasses, *J. Non-Cryst. Solids* 55 (1983) 293.
- [85] Z.F. Wu, N. Zhou, B. Mao, et al., Study of the mixed alkali effect on chemical durability of alkali silicate glasses, *J. Non-Cryst. Solids* 84 (1986) 468.
- [86] J.E. Tsuchida, F.A. Ferri, P.S. Pizani, et al., Ionic conductivity and mixed-ion effect in mixed alkali metaphosphate glasses, *Phys. Chem. Chem. Phys.* 19 (2017) 6594.
- [87] A. Hameed, Md. Shareefuddin, M.N. Chary, The mixed alkali effect in the  $\text{MgO-Li}_2\text{O-Na}_2\text{O-K}_2\text{O-B}_2\text{O}_3$  glass system, *Phys. Chem. Glasses: Eur. J. Glass Sci. Technol. B* 57 (2016) 227.
- [88] H. Jain, H.L. Downing, N.L. Peterson, The alkali effect in lithium-sodium borate glasses, *J. Non-Cryst. Solids* 64 (1984) 335.
- [89] A. Li, M.T. Wang, M. Li, Z.G. Liu, et al., The effect of mixed alkali on structural changes and ionic migration characteristics in zinc borate glasses, *Mater. Phys. Chem.* 217 (2018) 519.
- [90] C.J. Wilkinson, A.R. Potter, R.S. Welch, et al., Topological origins of the mixed alkali effect in glass, *J. Phys. Chem. B* 123 (2019) 7482.
- [91] J. Habasaki, C. León, K.L. Ngai, In: *The Mixed Alkali Effect Examined By Molecular Dynamics simulations*. in: Dynamics of glassy, Crystalline and Liquid Ionic Conductors, Springer, Cham, 2017, p. 459.
- [92] Y.T. Yu, M.Y. Wang, M.M. Smedskjaer, J.C. Mauro, et al., Thermometer effect: origin of the mixed alkali effect in glass relaxation, *Phys. Rev. Lett.* 119 (2017) 095501.
- [93] Y. Onodera, Y. Takimoto, H. Hijiya, et al., Origin of the mixed alkali effect in silicate glass, *NPG Asia Mater* 11 (2019) 75.
- [94] J. Swenson, S. Adams, Mixed alkali effect in glasses, *Phys. Rev. Lett.* 90 (2003) 155507.
- [95] H. Jain, N.L. Peterson, Impurity alkali diffusion in sodium-cesium silicate glasses, *J. Am. Ceram. Soc.* 66 (1983) 174.
- [96] K. Baral, A. Li, W.Y. Ching, Understanding the atomistic origin of hydration effects in single and mixed bulk alkali-silicate glasses, *J. Am. Ceram. Soc.* 102 (2019) 207.
- [97] S. Sen, F.V. Tolley, Effect of  $\text{Na}_2\text{O}/\text{K}_2\text{O}$  ratio on chemical durability of alkali-lime-silica glasses, *J. Am. Ceram. Soc.* 38 (1955) 175.
- [98] Y.Z. Sun, Y.A. Su, B.Y. He, Influence of the mixed alkali effect on the chemical durability of  $\text{Na}_2\text{O-TiO}_2\text{-SiO}_2$  glasses, *J. Non-Cryst. Solids* 80 (1986) 335.
- [99] A. Rodrigues, S. Fearn, M. Vialarigues, Mixed reactions: glass durability and the mixed-alkali effect, *J. Am. Ceram. Soc.* 102 (2019) 7278.
- [100] X.J. Wang, S. Fagerlund, J. Massera, et al., Do properties of bioactive glasses exhibit mixed alkali behavior, *J. Mater. Sci.* 52 (2017) 8986.
- [101] N.D. Afify, G. Mountjoy, Molecular-dynamics modeling of  $\text{Eu}^{3+}$ -ion clustering in  $\text{SiO}_2$  glass, *Phys. Rev. B* 79 (2009) 024202.
- [102] J. Lægsgaard, Dissolution of rare-earth clusters in  $\text{SiO}_2$  by Al codoping: a microscopic model, *Phys. Rev. B* 65 (2002) 174114.



- [103] L.R. Corrales, Free energy profiles of  $\text{Al}^{3+}$  and  $\text{La}^{3+}$  cation distribution in silica and soda silicate glasses, *J. Non-Cryst. Solids* 351 (2005) 401.
- [104] K. Arai, H. Namikawa, K. Kumata, et al., Aluminum or phosphorus co-doping effects on the fluorescence and structural properties of neodymium-doped silica glass, *J. Appl. Phys.* 59 (1986) 3430.
- [105] A. Monteil, S. Chaussedent, G. Alombert-Goget, et al., Clustering of rare earth in glasses, aluminum effect: experiments and modeling, *J. Non-Cryst. Solids* 348 (2004) 44.
- [106] F. Funabiki, T. Kamiya, H. Hosono, Doping effects in amorphous oxides, *J. Ceram. Soc. Jpn.* 120 (2012) 447.
- [107] S.F. Zhou, Q.B. Guo, H. Inoue, et al., Topological engineering of glass for modulating chemical state of dopants, *Adv. Mater.* 26 (2014) 7966.
- [108] A. Simo, J. Polte, N. Pfänder, et al., Formation mechanism of silver nanoparticles stabilized in glassy matrices, *J. Am. Chem. Soc.* 134 (2012) 18824.
- [109] A. Jha, S. Shen, M. Naftaly, Structural origin of spectral broadening of 1.5- $\mu\text{m}$  emission in  $\text{Er}^{3+}$ -doped tellurite glasses, *Phys. Rev. B* 62 (2000) 6215.
- [110] S.X. Shen, A. Jha, X.B. Liu, et al., Tellurite glasses for broadband amplifiers and integrated optics, *J. Am. Ceram. Soc.* 85 (2002) 1391.
- [111] S.F. Zhou, H.F. Dong, H.P. Zeng, et al., Broadband optical amplification in Bi-doped germanium silicate glass, *Appl. Phys. Lett.* 91 (2007) 061919.
- [112] N. Zhang, J.R. Qiu, G.P. Dong, et al., Broadband tunable near-infrared emission of Bi-doped composite germanosilicate glasses, *J. Mater. Chem.* 22 (2012) 3154.
- [113] S.F. Zhou, C.Y. Li, G. Yang, et al., Self-limited nanocrystallization-mediated activation of semiconductor nanocrystal in an amorphous solid, *Adv. Funct. Mater.* 23 (2013) 5436.
- [114] S.F. Zhou, N. Jiang, B.T. Wu, et al., Ligand-driven wavelength-tunable and ultra-broadband infrared luminescence in single-ion-doped transparent hybrid Materials, *Adv. Funct. Mater.* 19 (2009) 2081.
- [115] S.F. Wen, Y.P. Wang, B.J. Lan, et al., Pressureless crystallization of glass for transparent nanoceramics, *Adv. Sci.* 6 (2019) 1901096.
- [116] X.Y. Huang, H.H. Cheng, W. Luo, et al., Er-activated hybridized glass fiber for laser and sensor in the extended wavebands, *Adv. Opt. Mater.* (2021), doi:10.1002/adom.202101394.
- [117] Y.Z. Yu, Z.J. Fang, C.S. Ma, et al., Mesoscale engineering of photonic glass for tunable luminescence, *NPG Asia Mater.* 8 (2016) e318.
- [118] Q.Q. Ding, Y. Zhang, X. Chen, et al., Tuning element distribution, structure and properties by composition in high-entropy alloys, *Nature* 574 (2019) 223.



**Xu Feng** received the BS degree from South China University of Technology, Guangdong, China, in 2018. He is currently working toward the Doctor's degree at South China University of Technology, Guangdong, China. His current research interests focus on functional multi-component glass.



**Shifeng Zhou** received his PhD degree from Zhejiang University in 2008. From 2008 to 2009, he was with Hokkaido University as a postdoctoral researcher and then moved to Kyoto University as a JSPS postdoctoral fellow from 2009 to 2011. From 2011 to 2013, he was an associate professor at Zhejiang University. In 2013, he became a full professor at South China University of Technology. He is the recipient of the Gottardi Award of the International Commission on Glass and the Motoharu Kurata Award of the Ceramic Society of Japan. His primary research area is photonic materials and devices.